Bubbly flow velocity measurement in multiple scattering regime

Olivier Lombard[a],[*], Lilian D'Hondt[a],[b], Matthieu Cavaro[b], Serge Mensah[a], Cédric Payan[a]

[a] *Aix-Marseille Univ, CNRS (UPR 7051), Centrale Marseille, LMA, 13402 Marseille, France*
[b] *Commissariat à l'énergie atomique et aux énergies alternatives, Cadarache, DEN/DTN/STCP/LISM, Bat 202, 13108 Saint Paul Lez Durance, France*

A B S T R A C T

We propose a technique to measure the velocity of a bubble cloud based on the *coda* correlation. The method is founded on successive recordings of multiple scattered waves from a bubble cloud. Our model predicts the dependence between the correlation coefficient of these *coda* waves and the velocity of the bubble cloud under diffusion approximation. The Acoustic experiments are validated by simultaneous optical measurements in a water tank, with a good agreement between the acoustical and the optical methods (relative difference smaller than 7%). This technique can be transposed to any particle flow velocity problems involving multiple scattering effects in acoustics.

1. Introduction

Acoustic propagation in strongly scattering heterogeneous media has been widely studied for years [1–9]. In such media, the wave is multiply scattered as it encounters successively several heterogeneities. Consequently, transmitting an acoustic pulse through such a medium provides a typical signal generally showing a ballistic part at the first times of flight, followed by a multiply scattered coda, possibly lasting for a long time. When the scatterers are modeled as a random process, a wave propagating there could be described as a sum of a coherent and an incoherent field. A criterion to quantify the multiple scattering effect is $L > \ell_S$, where L is the distance over which the wave propagates in the medium and ℓ_S is the scattering mean free path. The scattering mean free path is a characteristic length between two scattering events. The local energy density of the incoherent field can be modeled as if the wave was a particle flux where no interference occurred, and thus obeys the Radiative Transfer Equation [10]. Furthermore, it could be simplified to a Diffusion equation, considering that the direction of the incoming wave is lost in the medium. The distance ℓ^* is called the transport mean free path and is the characteristic distance over which the incoherent field loses the memory of the direction of the incident wave. If $L > \ell^*$, it is common to observe a *coda*. When all the scatterers are identical, approximations give the scattering mean free path: $\ell_S = 1/n\sigma$, where n is the number of scatterers per unit of volume, and σ is the scattering cross section of scatterers. In bubbly media, the observation of a coda depends on the frequency f of the wave which probes the medium compared with the resonance frequency f_M of the bubbles. This resonance frequency is called Minnaert Frequency [11]. If $f \ll f_M$, the scattering cross section of the bubbles is very small, and it is very difficult to observe a multiple scattering event. If $f \approx f_M$, the scattering cross section is very large, and multiple scattering occurs. However, the absorption cross section is larger than the scattering cross section, and multiple scattering effects are not visible as *coda*. Finally, if $f \gg f_M$, bubbles still have a strong scattering cross section and a negligible absorption cross section and consequently, at this frequency, it is possible to observe a well developed *coda* [12].

The objective of this paper is to propose a technique for measuring the velocity of a bubble cloud driven by a flow, in a regime where multiple scattering effects are predominant. The most popular acoustic velocity measurement technique is the Doppler effect. However, when applying this technique, multiple scattering could be a problem. Most of the papers dealing with Doppler effect in scattering media assume no multiple scattering occurs [13]. In some other papers it is proposed to model the Doppler effect in Multiple Scattering regime using a Monte-Carlo simulation in acoustics [14] or in optics [15], and it is shown multiple scattering causes distorsion of the measured flow. Another paper proposes a technique using a beam-forming method [16], assuming that single scattering is predominant, that is to say, no multiple scattering occurs. In multiple scattering regime, another technique has been studied, using a coherent wave phase conjugation process [17]. This technique proposes a measurement based on the coherent part of the field, and may lose effectiveness when this coherent part becomes negligible. The technique developed in this paper is based on the sensitivity of the incoherent field to a slight perturbation in the medium. It uses only the incoherent part of a multiple scattered field to evaluate the bubble-cloud velocity measurement by studying the evolution of the incoherent field-field correlation coefficient. Our technique is closely related to Diffusive Wave Spectroscopy [18–22] in optics, Coda Wave Interferometry [23,24] in seismology and Diffusive Acoustic Wave Spectroscopy (DAWS) in acoustics [25–29].
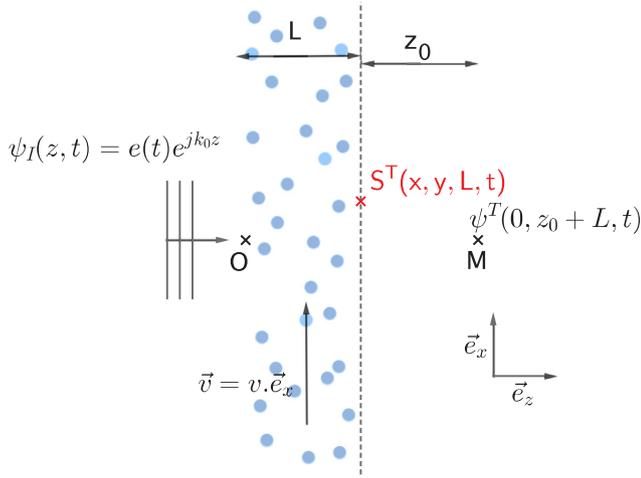

Fig. 1. Schematic diagram of the problem: An incident wave $\psi_I(z, t)$ propagates in a bubble cloud of thickness L. This bubble cloud is in uniform motion at velocity $\vec{v} = v \cdot \vec{e}_x$, perpendicular to the incident direction of the wave. $S^T(x, y, t)$ is the field at the bubble-cloud surface $z = L$, for an incident wave emitted at time T. The objective is to model the field at point M: $\psi^T(0, z_0 + L, t)$, resulting from the diffraction over a distance z_0 of $S^T(x, y, t)$ in the surrounding medium.

In the first part of this paper, we present a model, based on Diffusion Approximation, making the connection between the bubble velocity and the incoherent field-field correlation evolution. In the second part, we show our experimental configuration of the measurement, and finally, we present the experimental results to conclude about this method of velocity measurement.

2. Model

We consider a bubble cloud of thickness L, in which all the bubbles are moving at a velocity $\vec{v} = v \cdot \vec{e}_x$, as it is shown in Fig. 1. At the moment T, an incident wave, $\psi_I^T(z, t)$ is emitted at $z < 0$, and propagates in the direction $\vec{e}_z$ in the bubbly medium. The quantity of interest is $\psi^T(L + z_0, t)$, that is to say, the wave transmitted by the bubbly medium at the distance z_0 from its surface. Let us assume the Diffusion Approximation is verified, and thus the transmitted field has a coda. Because of the bubble displacement and multiple scattering, the two fields ψ^{T_1} and ψ^{T_2} resulting from the scattering of $\psi_I^{T_1}$ and $\psi_I^{T_2}$ have a very different coda temporal form. We assume our system is stationary, therefore the correlation coefficient of the signals ψ^{T_1} and ψ^{T_2} depends on $\tau_{12} = T_2 - T_1$, and it is noted $G(\tau_{12})$. The model studied here has the objective to clarify the relation between $G(\tau)$ and the bubble velocity v. The model assumes that the bubbles are motionless during wave propagation. If the bubbly medium was probed around Minnaert frequency, this approximation might not describe the reality, because the speed of sound in a bubbly medium around this frequency could be very low. However, this paper studies the interaction of an acoustic wave whose central frequency is higher than the Minnaert frequency. At this frequency, recent work has shown that the coherent field is described by the Independent Scattering Approximation [12]. This Model that neglects the correlation position and the loop of scattering predicts a group velocity not very different from the velocity in the surrounding medium. If the flow velocity is much smaller than the velocity in the surrounding medium, it is possible to assume that the bubbles are motionless during wave propagation.

The bubbly medium is modeled as a random process realization that is statistically spatially translation invariant in directions $\vec{e}_x$ and $\vec{e}_y$. The bubbly medium also has the property of spatial ergodicity, implying that all realizations of disorder can be observed at sufficiently different locations in the medium. Thus, the correlation coefficient is:

$$G(\tau) = \frac{\int < \psi^T(L + z_0, t)\psi^{T+\tau}(L + z_0, t) > dt}{\int < |\psi^T(L + z_0, t)|^2 > dt},$$
(1)

where $<...>$ means the averaged value over all bubble disorder realizations. The coefficient correlation is also, in the frequency domain:

$$G(\tau) = \frac{\int < \hat{\psi}^T(L + z_0, \omega)^*\hat{\psi}^{T+\tau}(L + z_0, \omega) > d\omega}{\int < |\hat{\psi}^T(L + z_0, \omega)|^2 > d\omega},$$
(2)

where $\hat{\psi}$ is the temporal Fourier Transform of ψ. Interactions between an acoustic wave and bubbles generate multiple scattering effects when the propagation length is longer than the scattering mean free path ℓ_e, which depends on the bubble concentration and the scattering cross section of each bubble. As the medium is modeled as a random process, the acoustic wave is the sum of its coherent and incoherent parts. If the thickness of the medium is longer than the transport mean free path, the incoherent field could be described by a random walk process, and it is possible to assume the local energy density is described by a Diffusion Equation. Under the diffusion approximation, the incoherent field at a position $\vec{r} = x \cdot \vec{e}_x + y \cdot \vec{e}_y + L \cdot \vec{e}_z$ on the sample surface can be modeled as a sum of replicas of the incident signal $e(t)$ [27]:

$$S^T\left(\vec{r}, L, t\right) = \sum_n A_n e\left(t - \tau_n(\vec{r})\right).$$
(3)

with $\tau_n(\vec{r})$, corresponding to the different times of flight through the bubble cloud and A_n being the pressure amplitude of the partial wave with time of flight $\tau_n(\vec{r})$. These times of flight depend on the spatial disorder of the bubbles and also on their size distribution. Consequently, times of flight τ_n are also random processes. The statistical translation invariance in $\vec{e}_x$ and $\vec{e}_y$ directions implies $\tau_n(\vec{r})$ are identically distributed whatever $\vec{r}$. If $\Delta\tau$ is the duration of the incident wave, we assume all the times of flight in an interval of length $\Delta\tau$, centered on the arrival time t_0, have an average magnitude $A(t_0)$. Thus the Fourier Transform of S^T in an interval $[t_0 - \Delta\tau/2; t_0 + \Delta\tau/2]$ is:

$$\hat{S}^T\left(\vec{r}, L, \omega\right) = A(t_0)\hat{E}(\omega) \sum_n e^{j\omega\tau_n(\vec{r})}$$
(4)

If the signal has a narrow bandwidth, which implies $\omega\Delta\tau \gg 1$, the mean value of S^T is zero, which is logical because it corresponds to the mean value of the incoherent part of the field. The mean value of the incoherent intensity is:

$$<|\hat{S}^T(\vec{r}, L, \omega)|^2 > = N_S|A(t_0)\hat{E}(\omega)|^2,$$
(5)

where $|A(\tau_0)|^2$ obeys a Diffusion Equation, under the Diffusion Approximation. N_S is the number of paths corresponding to the times of flight over the interval $[t_0 - \Delta\tau/2; t_0 + \Delta\tau/2]$. The correlation coefficient defined by Eq. (2) could be expressed as a function of the field at the sample surface S^T using the relation between $\hat{S}$ and $\hat{\psi}$. ψ^T results from the diffraction of S^T over the distance z_0 in the surrounding fluid. The relation between $\hat{S}^T$ and $\hat{\psi}$ is given by the Rayleigh-Sommerfeld integral [33]:

$$\hat{\psi}^T\left(L + z_0, \omega\right) = \frac{z_0}{j\lambda} \iint \hat{S}^T\left(x, y, L, \omega\right) \frac{e^{jk\sqrt{x^2+y^2+z_0^2}}}{x^2 + y^2 + z_0^2} dxdy.$$
(6)

The Fresnel Approximation makes it possible to simplify this relation:

$$\hat{\psi}^T\left(L + z_0, \omega\right) = \frac{e^{jkz_0}}{j\lambda z_0} \iint \hat{S}^T\left(x, y, L, \omega\right) e^{j\frac{k}{2z_0}\left(x^2+y^2\right)} dxdy.$$
(7)

In the experimental condition, the incident wave is generated by a transducer of finite size, and thus the surface support for the incident wave is also finite. In addition, let bubbles be in the near zone of the transducer. Thus, the acoustic beam is collimated and the field at the sample surface also has a finite aperture. We assume the spatial support

for the incident acoustic wave inscribes itself in a disk of radius a. In this case, the Fresnel approximation is verified if $z_0 \gg a$.

The spatial autocorrelation function $<S^{T*}(\vec{r_1}, L, \omega)S^T(\vec{r_2}, L, \omega)>$ depends on $\vec{r_2} - \vec{r_1}$ because of the statistical invariant property of the bubble cloud in the orthogonal direction to $\vec{e_z}$, and thus:

$$<S^T(\vec{r_1}, L, \omega)^* S^T(\vec{r_2}, L, \omega)> = N_S |A(t_0)E(\omega)|^2 \chi(\vec{r_2} - \vec{r_1}). \quad (8)$$

Then, all times of flight $\tau_n(\vec{r})$ are independent because of the diffusion approximation, and consequently the field at the sample surface can be modeled as a spatial white noise:

$$\chi(\vec{r_2} - \vec{r_1}) = U\delta(\vec{r_2} - \vec{r_1}), \quad (9)$$

where U is a constant. As a consequence of the bubble motion, S^T and $S^{T+\tau}$ verify:

$$S^{T+\tau}(x, y, L, \omega) = S^T(x - v\tau, y, L, \omega), \quad (10)$$

where it is expected that τ is greater than the duration of the transmitted signal. The spatial intercorrelation function between S^T and $S^{T+\tau}$ is:

$$<S^T(\vec{r_1}, L, \omega)^* S^{T+\tau}(\vec{r_2}, L, \omega)> = N_S |A(t_0)E(\omega)|^2 U\delta(x_2 - x_1 - v. \tau)\delta(y_2 - y_1). \quad (11)$$

Using Eq. (11) and Eqs. (2 and 7), the correlation coefficient defined at Eq. (2) is:

$$G(\tau) \approx \iint_\Sigma e^{-j\frac{\omega_c}{c_0}\frac{xv\tau}{z_0}} dx dy, \quad (12)$$

where ω_c is the angular central frequency of the incident signal and Σ is the spatial support of the field at the sample surface. If we suppose the spatial support of S^T and $S^{T+\delta T}$ is a disk of radius a, the correlation coefficient is:

$$G(\tau) = 2\frac{J_1(\alpha\tau)}{\alpha\tau}, \quad (13)$$

where α is:

$$\alpha = \frac{a}{z_0}\frac{v}{c_0}2\pi f_c. \quad (14)$$

The approximation made at Eq. (12) is that $J_1(\alpha\tau)$ varies slowly over this useful bandwidth of the incident signal $E(\omega)$ and thus its averaged value over the useful bandwidth is equal to its value at the central frequency of the signal. It is interesting to observe that, while the field at the bubble cloud surface is a spatial white noise, after a propagation distance z_0 and as a consequence of the diffraction on this distance, a correlation between two transmitted fields separated by a time τ does exist. This correlation is a consequence of the finite size of the spatial support of the field. A limit case is to consider that when $a \gg z_0$ the diffraction effect is negligible, and the field remains a spatial white noise after a propagation distance z_0. Two transmitted fields separated by a time τ, in this case, are uncorrelated, and $G \to 0$. If $a \ll z_0$, the degradation of the angular resolution, due to the diffraction, decreases the difference perceived between the two transmitted fields separated by a time τ. Thus, on the one hand, the motion of bubbles during a time τ tends to reduce the correlation between two transmitted waves separated by the same time. On the other hand, the finite size of the spatial support of the field tends to keep a correlation between those fields. The decay of G as a function of τ is a consequence of the superposition of those two antagonistic effects. These theoretical results are an application of the Van-Cittert and Zernicke theorem [30,31].

The model proposes a relation between the correlation coefficient and the bubble velocity v. A measurement of the correlation coefficient as a function of τ could therefore be a measurement of the uniform velocity of the scatterers v. The objective of the next part is to show experimental results giving a confirmation of this model and to propose a velocity measurement technique.
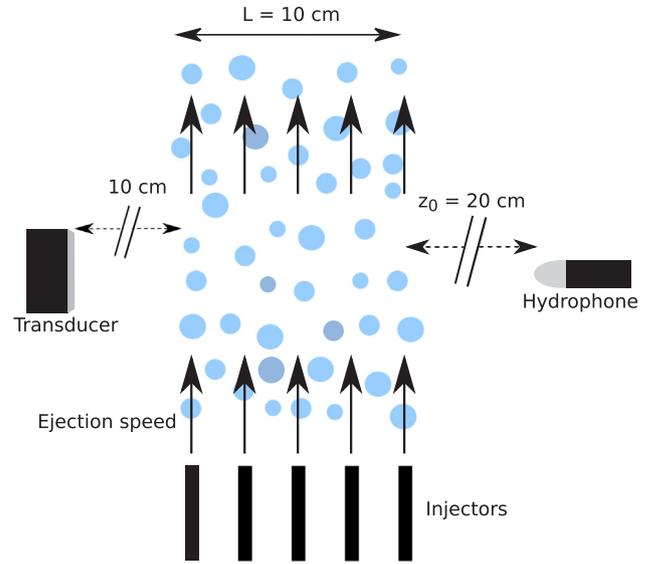

Fig. 2. Experimental setup: Five injectors inject bubbles in the surrounding water at an ejection speed $\vec{v}$. The bubbles move at a velocity equal to the ejection speed. A transducer emits an ultrasonic plane wave. A hydrophone records the wave transmitted by the bubbly medium at the distance $z_0 = 20.0 \pm 1.0$ cm from the bubbly sample surface.

3. Experimental procedure

3.1. Material and methods

Fig. 2 shows the experimental setup: in a 1 m³ water tank, a transducer emits an acoustic wave that propagates in a bubbly medium. A hydrophone records the transmitted wave at the distance $z_0 = 20.0 \pm 1.0$ cm beyond the bubbly medium. The uncertainty of 1.0 cm comes from the uncertainty of the position of the surface of the bubbly medium.

The bubbly medium is obtained using a radial divergence vein: Over-saturated water is injected through specific injectors with fast divergent outlet. The rapid relaxation that is induced creates a cavitation pocket which collapses, and since the water is over-saturated, stable micro-bubbles remain. Then, the fluid containing the bubbles is ejected in the water tank by five injectors. This generation process creates a flow, driving the bubbles. Ultrasonic measurements are made in a region near the injector outlets, where we can assume that, on the one hand the flow is uniform, on the other hand, all the bubbles are driven by the flow at the velocity $\vec{v}$, equal to the flow velocity. The ultrasonic measurements are made to assess this velocity $\mathbf{v}$. A polydisperse bubbly medium is thereby produced. Optical measurement are made on the medium to estimate its radius distribution - plotted in Fig. 3 - and its gas fraction, using an immersed camera *Baumeur TXG50*. These optical measurements are performed using successive pictures of the bubble cloud at different times and positions. The location corresponds with acoustical measurement zone which is close to the injector outlets. A photo of the bubbly medium is showed in the inset of Fig. 3. The radius distribution function can be approximated using a gamma function with a mean radius of $R_0 = 14.6$ μm and a standard deviation $\sigma = 6.7$ μm. The gas fraction is measured around $\phi_0 = 10^{-4}$. The size of the bubbly medium is 50 cm × 10 cm × 10 cm.

A piezoelectric transducer (Olympus A395S, with a central frequency of 2.25 MHz and 38 mm in diameter), emits a pulse with a Gaussian envelope, containing 8 periods of a sinusoidal signal centered at 1.2 MHz within the transducer bandwidth limits. This in order to probe the medium at a frequency at which bubbles have a larger scattering cross section, and thus to increase the multiple scattering
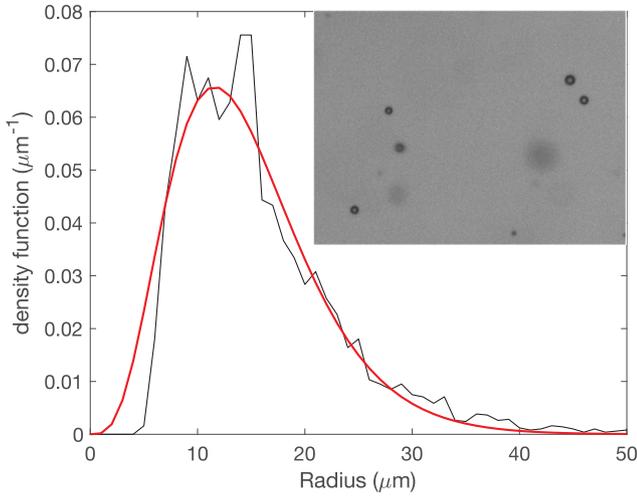
Fig. 3. Black line: Bubble radius distribution function in the cloud, produced in our experiments. Red line: Fit with a Γ function with mean radius $R_0 = 14.6\ \mu m$ and standard deviation: $\sigma = 6.7\ \mu m$. Inset: Photography of the bubbly medium. (For interpretation of the references to colour in this figure legend, the reader is referred to the web version of this article.)

effects. The transducer near field distance is around 30 cm at 1.2 MHz, therefore the beam propagating in the bubbly medium is collimated, in particular at the sample surface. The transducer is connected to a tension generator working in burst regime. As the velocity of the cloud is not tunable in our experiments, three independent measurements are performed changing the pulse repetition frequency (PRF), set at 100, 200 and 400 Hz. That means that we have an acoustical signature of the cloud every $dT_{100} = 10\ ms$, $dT_{200} = 5\ ms$ and $dT_{400} = 2.5\ ms$. This procedure is somewhat equivalent to keep a constant PRF with a bubble cloud moving at different velocities.

A hydrophone (RESON TC4038) records the transmitted field at a distance $z_0 = 20\ cm$. The transmitted wave is recorded every dT_{PRF}.

To test the hypothesis bubble motionlessness during the wave propagation in the medium, we compare the group velocity of the coherent field with the flow velocity, assuming that the group velocity gives an order of magnitude of an effective sound velocity in the bubbly medium. The Independent Scattering Approximation in the polydisperse case predicts the following wave number [32]:

$$k^2 = k_0^2 + 3\phi_0 \int \frac{f_0(R)}{R^3} \mathrm{pdf}(R) dR, \tag{15}$$

where $\mathrm{pdf}(R)$ is the function plotted in Fig. 3, and $f_0(R)$ is the forward scattering function of a bubble of radius R. This approximation predicts a group velocity around $1420\ m.s^{-1}$ for such bubbly medium, and for a wave at a central frequency around 1 MHz, which is much higher than the flow velocity, which is around $0.1\ m\,s^{-1}$. The hypothesis that assumes bubble motionlessness during wave propagation is consistent with this experiment.

Finally, the transport mean free path is:

$$\ell_e = \frac{1}{\Im(k)}$$
$$\ell^* = \frac{\ell_e}{1 - <\cos>} \tag{16}$$

where $<\cos>$ is the cosine of all scattering angles averaged on the differential scattering cross section. At 1.2 MHz, we get a transport mean free path of 2 cm. The thickness of the bubbly medium over which the acoustic wave propagates is $L = 10\ cm$. It is equal to 5 transport mean free paths in these conditions, which is enough to observe an incoherent regime described by the Diffusion Approximation.

3.2. Results and analysis

This part details the measurements and the data processing giving the velocity of the bubble cloud for the repetition frequency of 200 Hz. Fig. 4.c shows four arbitrarily chosen signals acquired at the repetition frequency of 200 Hz, after propagation through the bubbly sample of the incident wave $\psi_I^T(t)$ represented under its temporal (Fig. 4a) or spectral (Fig. 4b) form. Each transmitted signal, recorded at a time T, corresponds to one bubble disorder realization. The signal coda, well developed, is characteristic of the bubble disorder. In this experiment, we record $N = 2000$ signals, every $dT_{200} = 5\ ms$, noted $s_i(t)$. The total duration of the acquisition is 10 s.

3.2.1. Validity of the diffusion approximation

Before working on the correlation coefficient to validate the model, it is necessary to check whether the diffusion approximation is verified in this experiment. When the diffusion approximation is verified, the local energy density W is described by a diffusion equation governed by a coefficient D. As described in reference [2,4,5,12], the finite thickness of our sample can be taken into account by adding boundary conditions to the diffusion equation describing W, leading to a modal decomposition of W:

$$W\left(z, t\right) = \sum_{m=1}^{\infty} A_m \sin\left(\frac{m\pi\left(z + \frac{2\ell^*}{3}\right)}{L + \frac{4\ell^*}{3}}\right) e^{-D\left(\frac{m\pi}{L + \frac{4\ell^*}{3}}\right)^2 t}. \tag{17}$$

Each mode m exponentially decreases with a characteristic time inversely proportional to m^2:

$$\tau_{D_m} = \frac{(L + 4\ell^*/3)^2}{m^2\pi^2 D} \tag{18}$$

Thus, for long enough times, the first diffusive mode dominates all others, and the local energy density decreases exponentially with the characteristic time τ_{D_1}. Experimentally, we measure the acoustic intensity of the incoherent wave, which is the average value of the Poynting vector $\overrightarrow{J} = -D\overrightarrow{\nabla}W$. Therefore, the intensity of the incoherent field also exponentially decreases with a characteristic time τ_{D_1} under the diffusion approximation and with the appropriate boundary conditions. To estimate the incoherent intensity, we take part of both the spatial ergodicity and the spatial translation invariance of the medium. In our experiment, the hydrophone is motionless but the bubbles are moving. The ergodicity implies that all our recorded signals are representative patterns of the bubble disorder realizations. The incoherent intensity is estimated by:

$$<I_e(t)> = \frac{1}{N} \sum_{i=1}^{N} \left| HT\left(s_i(t)\right) \right|^2, \tag{19}$$

where $HT(s_i)(t)$ signifies the Hilbert Transform of the signal $s_i(t)$.

Fig. 5 shows the temporal evolution of the incoherent intensity averaged over bubble disorders, obtained using the estimator given at Eq. (19). We observe the first arrival time of flight from $275\ \mu s$ to $280\ \mu s$. In this interval, the incoherent intensity is better described by a radiative transfer equation [10] and does not obey a diffusion equation. Between $280\ \mu s$ and $320\ \mu s$, the incoherent intensity decreases as an exponential function, thus we can conclude the Diffusion Approximation is well verified over this interval [2,9,12].

Thus, it is possible to apply our model showed in part II on the interval 280–$320\ \mu s$, where the profile of the intensity is well described by a diffusion equation associated with boundary conditions. This interval is wide enough so that it is longer than the temporal duration of the incident field. Therefore we can study the evolution of the correlation coefficient of the recorded signals, and thus obtain an estimator of its time evolution.
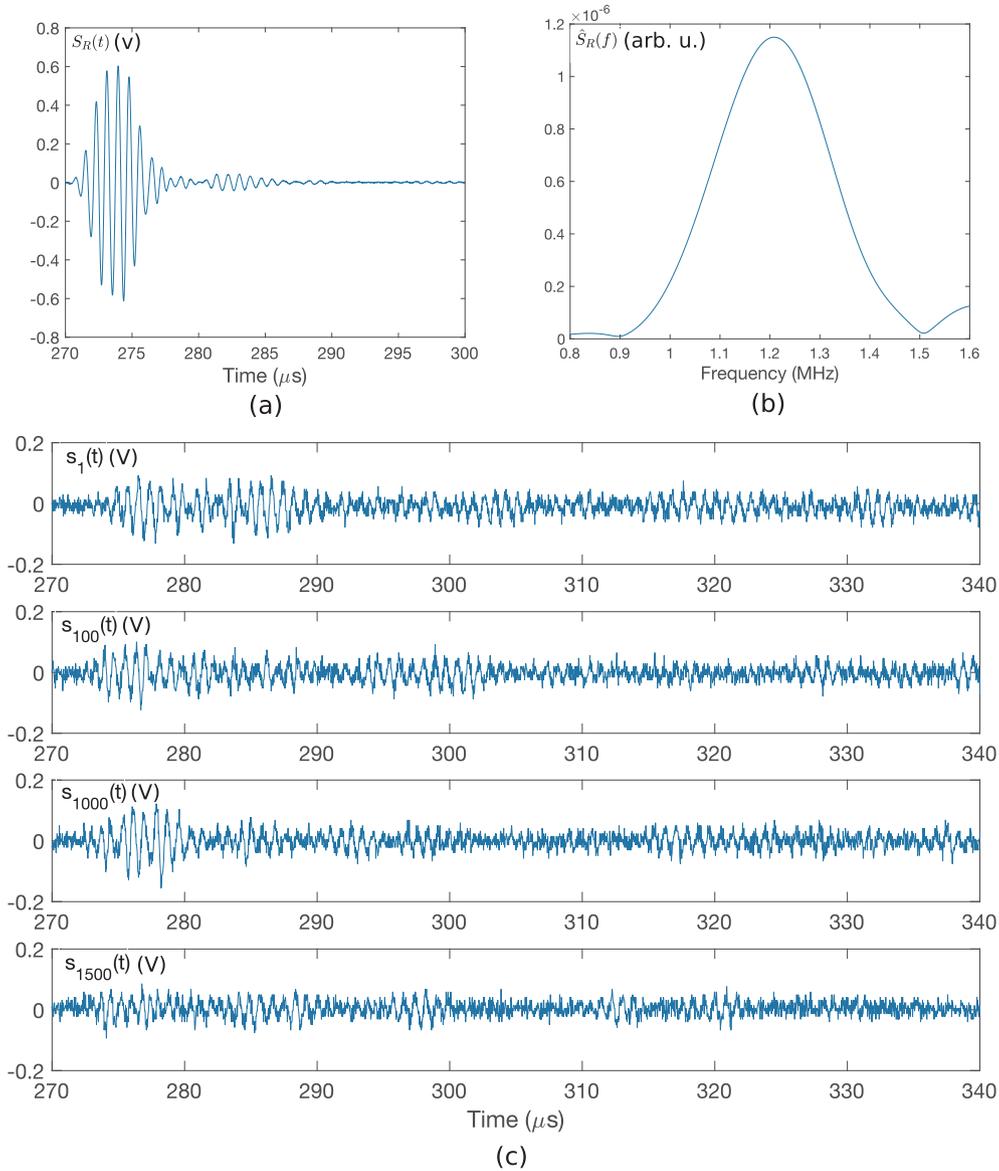
Fig. 4. (a) Reference signal recorded by the hydrophone after 40 cm propagation in the water. (b) Spectrum of the reference signal. (c) Four signals recorded by the hydrophone at different times, with 10 cm propagation in the bubble cloud. The transducer emit a signal every $dT_{200} = 5$ ms. The hydrophone is at $z_0 = 20$ cm beyond the bubble cloud surface and records the transmitted wave at every time dT_{200}. Temporal signals are in Volts, and the spectrum is in arbitrary units.

3.2.2. Correlation coefficient estimation

Using the 2000 recorded signals, we need to find a good estimator for the correlation coefficient between two recorded signals separated by $\tau = n \times dT$, with $dT_{200} = 5$ ms. The window used to evaluate the Fourier Transform of the signals is centered at $t_0 = 295\ \mu s$, to be under Diffusion Approximation. The size of the window is equal to the size of the incident field: $\Delta t_0 = 8.5\ \mu s$. The correlation coefficient between two signals separated by $\tau = n \times dT_{200}$ and over one bubble disorder is:

$$G_p(ndT_{200}) = \frac{\int s_p(t) s_{n+p}(t) dt}{\sqrt{\int s_p(t)^2 dt}\sqrt{\int s_{n+p}^2(t) dt}}. \tag{20}$$

Because of the poor signal to noise ratio, it is necessary to take the noise into account when calculating the correlation coefficient. The noise level N_p of the p recorded signals is quantified with the intensity of the recorded signal before $t = 270\ \mu s$.

$$G_p(ndT_{200}) = \frac{\int s_p(t) s_{n+p}(t) dt - N_p \times \delta_{n,0}}{\sqrt{\int s_p(t)^2 dt - N_p}\sqrt{\int s_{n+p}^2(t) dt - N_{n+p}}}, \tag{21}$$

where $\delta_{n,0}$ is the Kronecker symbol equal to 1 if $n = 0$ and equal to 0 in the other cases. To compare the experimental results with the model, this correlation coefficient is averaged over several realizations in the following way. Considering the time interval -100 ms $< \tau < 100$ ms, this means we need to use $K = 41$ signals to calculate this correlation coefficient over one disorder realization of the bubbles. Consequently, we can estimate this correlation coefficient over $P = 49$ bubble disorder realizations:

$$<G(ndT_{200})> = \frac{1}{P}\sum_{l=1}^{P} G_{20l+1}(ndT_{200}), \quad -\frac{K}{2} \leqslant n \leqslant \frac{K}{2}. \tag{22}$$

The correlation coefficient estimated by Eq. (22) is shown in Fig. 6. Error bars are evaluated using:

$$\sigma_G = \frac{1}{\sqrt{P}}\left(\frac{1}{P}\sum_{l=1}^{P}(G_{20l+1}(ndT_{200}) - \langle G(ndT_{200})>)^2\right)^{1/2} \tag{23}$$

The correlation coefficient is well described by an analogous function that is given at Eq. (13) over the interval -50 ms $\leqslant \delta T \leqslant 50$ ms. The
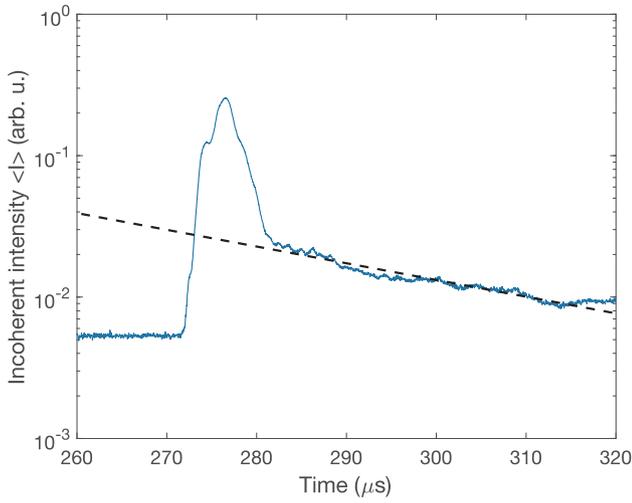
Fig. 5. Incoherent intensity $<I>$ in arbitrary units, obtained with the estimator given at Eq. (19) (blue line). Experimental results are fitted with an exponential function e^{-t/τ_D} (dotted black line). (For interpretation of the references to colour in this figure legend, the reader is referred to the web version of this article.)
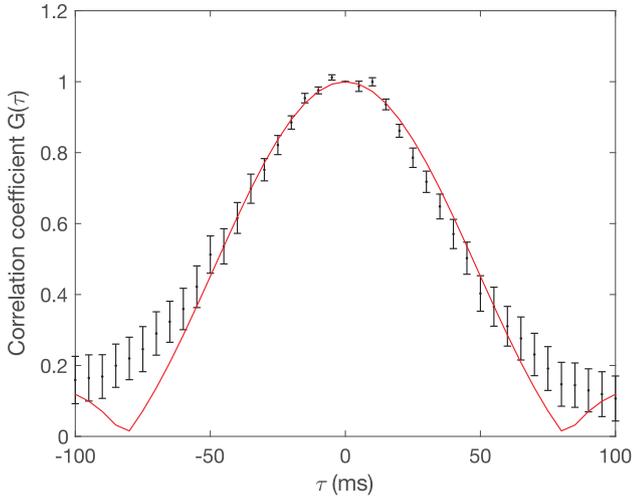

Fig. 6. Experimental estimation of the correlation coefficient $G(\tau)$ between two recorded signals separated by a time τ. This correlation coefficient is obtained averaging $P = 49$ bubble disorder realizations.

model describes well the time evolution of the correlation coefficient over this interval. For the higher times of flight, the decorrelation rate between two signals is lower than predicted by the model. To get the analytical function of the correlation coefficient, we inverse the problem by minimizing the cost function:

$$F(\alpha) = \int_{-T}^{T} \left| 2\frac{J_1(\alpha\delta T)}{\alpha\delta T} - <G\left(\delta T\right)> \right| d\delta T \quad \text{with} \quad T = 60 \text{ ms.}$$

(24)

The minimization procedure gives $\alpha = 47.7 \pm 1.3 \text{ s}^{-1}$. With Eq. (14) it is possible to evaluate the velocity v of the bubbles. The parameters $z_0 = 20, 0 \pm 1, 0 \text{ cm}$ and $c_0 = 1490 \text{ m·s}^{-1}$ are known. We assume the spatial support of the field at the bubble cloud is a disk of the same radius as the transducer, so $a = 1.90 \pm 0.10 \text{ cm}$. This is due to the fact that the near field distance is around 25 cm, and the bubbly medium surface is at 30 cm from the transducer. This method gives the following bubble velocity: $v_{200} = 9.40 \pm 0.38 \text{ cm·s}^{-1}$. We detailed the experiments made at the repetition frequency of 200 Hz. Using the same experimental acquisition and data processing, the other experiments made with repetition frequencies of 100 Hz and 400 Hz yield respectively these following bubble velocities: $v_{100} = 9.49 \pm 0.41 \text{ cm·s}^{-1}$ and

$v_{400} = 9.09 \pm 0.39 \text{ cm·s}^{-1}$.

The acoustical assessment was confirmed by an optical measurement. A video-camera records an image during an exposure time of 2.3 ms. The bubbles are moving during this duration, and the final image shows a distorted bubble between its initial and final position. We can deduce the distance traveled by the bubbles during the exposure time, and consequently, their velocity. We measured the velocities of 164 bubbles, we found a mean velocity value of $\bar{v} = 8.9 \text{ cm·s}^{-1}$ and a standard deviation $\sigma_v = 3.5 \text{ cm·s}^{-1}$. Consequently, the velocity obtained by the optical measurement is $v = 8.90 \pm 0.28 \text{ cm·s}^{-1}$ which confirms the acoustical measurement of the bubble velocity proposed in this paper.

This measurement technique is robust regarding a change of the PRF frequency, that demonstrates it is also robust regarding a change of the bubble cloud velocity. In practice, the measurements aim at interpolating the correlation coefficient which corresponds to the function determined at the Eq. (13). In that relation, experimental values are fixed by the user such as the transducer radius a, the distance z_0 and the central frequency f_c or are related to the surrounding medium through c_0, and the velocity of the bubble cloud. These data provide the parameter α_{real} (Eq. (14)). Ultrasonics measurements aim at measuring the correlation coefficient, the inversion of which gives an estimation α_{est}. To evaluate the efficiency of our method, we calculate $G(\alpha_{\text{real}}\delta T)$ given by the Eq. (13), for three values of α_{real}. The calculation is performed at the times $\delta T = ndT_{\text{PRF}}, -50 < n < 50$. A centered Gaussian noise with a standard deviation 0.05, is added to $G(\alpha_{\text{real}}\delta T)$ to mimmick the experimental noise. Then, the function $G(\alpha_{\text{real}}\delta T)$ is inverted. This process is repeated for different values of dT_{PRF}. The relative error given by $|\alpha_{\text{EST}} - \alpha_{\text{real}}|/\alpha_{\text{real}}$, is plotted in Fig. 7 as a function of the dimensionless repetition period $\alpha_{\text{real}} \times dT_{\text{PRF}}$. The relative error increases drastically when $\alpha_{\text{real}} \times dT_{\text{PRF}} > 3$. Therefore, the user must adjust the repetition frequency to verify the inequality:

$$\alpha_{\text{real}} \times dT_{\text{PRF}} < 3.$$

(25)

If this condition is fulfilled, the correlation coefficient can be inverted using the procedure detailed in this paper, to obtain an estimate of the bubble cloud velocity.

4. Conclusion

The present study shows that it is possible to measure particle flow velocity, using the coda of a transmitted acoustic wave. It is shown that the time decorrelation of successive multiply-scattered waves depends on the velocity of the scatterers. Experimental validations were
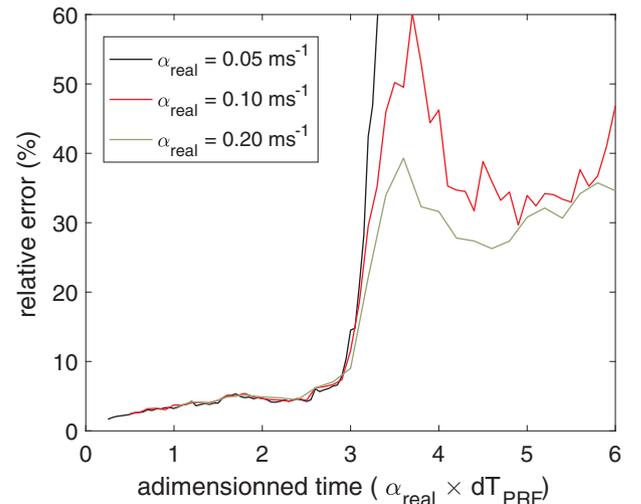

Fig. 7. Relative error between $|\alpha_{\text{real}} - \alpha_{\text{est}}|/\alpha_{\text{real}}$ as a function of the dimensionless repetition period.

conducted in a tank filled with water and containing a cloud of moving bubbles. These results of this velocimetry method are confirmed by closely agreeing optical measurements. This technique is different from previous techniques using more the coherent part of a field [17]. Furthermore, if the operating condition is that most of the field is incoherent, the classical technique using the Acoustical Doppler Velocimetry loses effectiveness and this technique could be a good resort to velocity measurement. This method could also be efficient for bubbly flow velocity measurement through an opaque pipe, using piezotransducers placed on the surface. Indeed, the estimation of the correlation coefficient, which determines the flow velocity will not be affected by the presence of the pipe while the contribution of the latter remains unchanged over successive measurements.

Current efforts aim at improving an experimental application using a multi-channel probe than could be directly immersed into the medium in order to reduce uncertainties.

References

[1] A. Ishimaru, Wave Propagation and Scattering in Random Media, Academic Press, New York, 1978.
[2] J.H. Page, H.P. Schriemer, A.E. Bailey, D.A. Weitz, Phys. Rev. E 52 (1995) 3106.
[3] A. Lagendijk, B.A. Van Tiggelen, Phys. Rep. 270 (1996) 143.
[4] J.H. Page, H.P. Schriemer, I.P. Jones, Ping Sheng, D.A. Weitz, Physica A 241 (1997) 64–71.
[5] A. Derode, A. Tourin, M. Fink, Phys. Rev. E 64 (2001) 036605.
[6] S. Skypetrov, B. Van Tiggelen, NATO Science Series vol. 107, Kluwer, Dordrecht, 2003.
[7] A. Derode, V. Mamou, A. Tourin, Phys. Rev. E 74 (2006) 036606.
[8] M.A. Ouarabi, F. Boubenider, A.S. Gliozzi, M. Scalerandi, Phys. Rev. B 94 (2016) 134103.
[9] B. Tallon, T. Brunet, J.H. Page, Phys. Rev. Lett. 119 (2017) 164301.
[10] A. Lagendijk, B.A. Van Tiggelen, Phys. Rep. 270 (1996) 143.
[11] M. Minnaert, Philos. Mag. (1933) 235–248.
[12] O. Lombard, N. Viard, V. Leroy, C. Barrière, Euro. Phys. J. E 41 (2018) 18.
[13] D. Censor, V.L. Newhouse, J. Acoust. Soc. Am. 83 (6) (1988) 2012–2019.
[14] A. Battaglia, S. Tanelli, IEEE Trans. Geosci. Rem. Sens. 49 (1) (2011).
[15] J. Kalkman, A.V. Bykov, D.J. Faber, T.G. Leeuwen, Opt. Exp. 18 (4) (2010).
[16] B. Saint-Michel, H. Bodiguel, S. Meeker, S. Manneville, Phys. Rev. Appl. 8 (2017) 014023.
[17] P.N. Shirkovskiy, N.V. Smagin, V.L. Preobrazhenski, P. Pernod, Acoust. Phys. 1 (2016) 62.
[18] G. Maret, P. Wolf, Z. Phys. B: Condens. Matter 65 (1987) 409.
[19] D.J. Pine, D.A. Weitz, P.M. Chaikin, E. Herbolzheimer, Phys. Rev. Lett. 60 (1988) 1134.
[20] D. Bicout, E. Akkermans, R. Maynard, J. Phys. I France 1 (1991) 471–491.
[21] D. Bicout, G. Maret, Physica A 210 (1994) 87–112.
[22] J. Crassous, Euro. Phys. J. E 23 (2007) 45.
[23] R. Snieder, Pure Appl. Geophys. 163 (2006) 455–473.
[24] C. Payan, V. Garnier, J. Moysan, Appl. Phys. Lett. 94 (2009) 011904.
[25] J.H. Page, M.L. Cowan, D. Weitz, Physica B 279 (2000) 130.
[26] M.L. Cowan, I.P. Jones, J.H. Page, D.A. Weitz, Phys. Rev. E 65 (2002) 066605.
[27] V. Leroy, A. Derode, Phys. Rev. E 77 (2008) 036602.
[28] E. Larose, T. Planes, V. Rossetto, L. Margerin, Appl. Phys. Lett. 96 (2010) 204101 1–3.
[29] V. Rossetto, L. Margerin, T. Planès, E. Larose, J. Appl. Phys. 109 (2011) 034903 1–11.
[30] R. Mallart, M. Fink, J. Acoust. Soc. Am. 90 (1991) 2718.
[31] F. Gori, m. Santarsiero, R. Borghi, G. Piquero, Opt. Lett. 25 (17) (2000) 1291–1293.
[32] V. Leroy, A. Strybulevych, J.H. Page, M.G. Scanlon, J. Acoust. Soc. Am. 123 (4) (2008) 1931–1940.
[33] E. Wolf, E.W. Marchand, J. Opt. Soc. Am. 54 (1964) 587.